# Analytical Methods



### **PAPER**

View Article Online
View Journal | View Issue



Cite this: Anal. Methods, 2023, 15, 482

# Portable, low-cost, Raspberry Pi-based optical sensor (PiSENS): continuous monitoring of atmospheric nitrogen dioxide†

Ernesto Saiz, (1) \*a Ivana Banicevic, b Sergio Espinoza Torres, (10) c Salma Bertata, a Gino Picasso, c Matthew O'Brien (10) \*a and Aleksandar Radu\*d

We have developed a sensing system that utilizes a low-cost computer (Raspberry Pi) and its imaging camera as an optical sensing core for the continuous detection of  $NO_2$  in the air (PiSENS-A). The sensor is based on colour development as a consequence of the interaction of the gas with an absorbing solution. The PiSENS-A is thoroughly calibrated over the hourly mean which is used as one of the key metrics in evaluating air quality. The calibration was performed in the range of  $0 < [NO_2] < 476 \,\mu g \,m^{-3}$  chosen to contain the threshold used to determine compliance to the UK's Air Quality Standard Regulations (2010) expressed as a maximum of 18 permitted exceedances of  $[NO_2]_{hourly mean} = 200 \,\mu g$  per  $m^3$  per year. Lab-based measurements were evaluated against UV-vis. The average precision expressed as a relative standard deviation was: RSD% = 2.8%, while the correlation of mock samples was excellent (Pearson's r = 1.000). Field-based measurements were evaluated against chemiluminescence-based instrument exhibiting a correlation coefficient of  $R^2 = 0.993$ . The PiSENS-A was also deployed as an independent air quality analyser at the Keele University campus.

Received 5th September 2022 Accepted 22nd December 2022

DOI: 10.1039/d2ay01433e

rsc.li/methods

#### Introduction

Today's world is insatiable for information. The demand to monitor and control all aspects of the environment in real-time is brought about by environmental, health, safety, and security concerns. Monitoring of chemically-relevant information is thus essential in these efforts. However, obtaining reliable, robust chemical information relevant for any of the aforementioned areas still very much depends on expensive, bulky, and lab-based instruments that require highly trained personnel for their operation which hinders their applicability to point-ofcare (POC) applications. 1,2 Advances in Information Technologies (IT) coupled with technologies for simplification and miniaturization of chemical sensors have led to the development of very interesting concepts for data collection and transmission in health and environmental applications.<sup>3,4</sup> Furthermore, advances in digital imaging technology have allowed the programming of computers to interpret and

Low-cost, single-board computers such as the Raspberry Pi<sup>7</sup> offer exciting opportunities to exploit computer vision in a variety of fields of chemical sciences. They can utilize versatile open source programming languages such as Python (and its available libraries) and thus offer an opportunity to modify and adapt protocols. For example, a Raspberry Pi coupled with an imaging camera has been used by O'Brien *et al.* to automate organic synthesis,<sup>8,9</sup> while Luka *et al.* have developed colourimetric sensors for the determination of pH and NO<sub>2</sub><sup>-</sup> concentration with a correlation coefficient of *R*<sup>2</sup> 0.998 and 0.999.<sup>10</sup>

We are working on the development of Raspberry Pi-based, portable devices for rapid and *in situ* determination of analytes relevant for bio-environmental analysis (PiSENS).

This paper focuses on the description of the version suitable for the determination of air quality hence named PiSENS-A. A forthcoming publication demonstrates a version suitable for the determination of water/soil quality utilizing polymer membrane-based optodes hence named PiSENS-O.

understand the visual world. Computer vision approaches enable the use of cost-effective and high-resolution cameras for colourimetric analysis in, for example, remote areas as well as the exchange of data from such POC tests almost instantaneously using, for example, smartphones.<sup>5</sup> More recently, the inclusion of cloud computing offers unprecedented opportunities for instantaneous data transmission even in resource-limited settings and remote areas, enabling intervention when required.<sup>6</sup>

<sup>&</sup>lt;sup>e</sup>Lennard-Jones Laboratories, Birchall Centre, Keele University, Keele, Staffordshire, ST5 5BG, UK. E-mail: e.saiz.val@keele.ac.uk; m.obrien@keele.ac.uk

<sup>&</sup>lt;sup>b</sup>Faculty of Technical Sciences, University of Montenegro, Montenegro

<sup>\*</sup>Laboratory of Physical Chemistry Research, Faculty of Sciences, National University of Engineering, Av. Tupac Amaru 210, Lima 25, Peru

<sup>&</sup>lt;sup>d</sup>School of Chemistry, Joseph Banks Laboratories, University of Lincoln, Green Lane, Lincoln, LN6 7DL, UK. E-mail: aradu@lincoln.ac.uk

<sup>†</sup> Electronic supplementary information (ESI) available. See DOI: https://doi.org/10.1039/d2ay01433e

For a demonstration of the utility of PiSENS-A, we focused on the rapid determination of NO2 in the air. NO2 is chosen as a major indicator of air quality. According to WHO, air pollution kills an estimated seven million people worldwide every year.11 Recently, a nine-year-old from London became the first person in the UK to have air pollution listed as the cause of death on their death certificate after an inquest into the child's death found levels of NO2 and PM2.5 near her home exceeding WHO and EU guidelines thus affecting her severe asthma.12

Since the principal sources of NO2 pollution are mobile (motor vehicles)13 capturing acute and localized incidents is very important but also makes spatio-temporal analysis quite difficult. Moreover, NO2 concentration can vary due to variations in wind speed and direction, rain, chemical sinks and sources, etc.14

Different methods are available to measure NO2 concenchemistry15 traditional wet to from chromatography,16-18 fluorescence,19,20 electrochemical sensors,21-23 and semiconductor gas sensors.24 Chemiluminescent methods<sup>25,26</sup> have established themselves as reference methods that governmental agencies such as the UK's Department of Environment, Food, and Rural Affairs (DEFRA) are using for the development of air quality policies.27 However, it requires high capital and operating costs. In recent years, there have been different attempts to develop low-cost devices to monitor NO2 in the air. Some devices are portable and can be applied at the POC but in two steps: sample collection and then colour analysis.28-30 In other cases, they are devices with high spatio-temporal resolution31-33 but with recurring issues with precision and reliance on expensive instrumentation for data acquisition and transmission.

In order to address the issues of cost, portability and instantaneous analysis, PiSENS-A was largely built using materials that can be found in a DIY shop while utilizing a Raspberry Pi and its imaging camera for data acquisition and processing. We utilize the traditional Saltzman reaction for capturing NO<sub>2</sub> from the air which results in colour development upon contact with a suitable absorbing solution.15 We also used a 3D printer for the construction of a few additional specific pieces, while the data acquisition and processing are driven by an in-house written Python script thus keeping the cost low and allowing for potential future modifications. While we acknowledge the limitations of the methodology relying on an absorbing solution, we decided that its combination with Raspberry Pi-based detection/analysis presents an optimal balance between cost, simplicity of construction and operation, and offered spatiotemporal resolution. Herein, we demonstrate that the PiSENS-A allowed data acquisition with a high temporal resolution and offered excellent portability of the single utilized device. However, we are confident that the low construction and operation costs and utilization of the computing power of Raspberry Pi open the possibility for the production and installation of several devices while integrating them into powerful sensing networks.

## **Experimental**

#### Reagents

In this study, all the chemicals were of analytical grade. N-1-Naphthylethylenediamine dihydrochloride with >98% purity, sulfanilic acid with >99% purity, and sodium nitrite with ≥97% purity were purchased from Sigma-Aldrich (Dorset, UK). Glacial acetic acid with ≥99% purity was purchased from Fisher Scientific (Loughborough, UK).

#### Absorbing reagent and solutions preparation

To prepare the absorbing reagent we first prepared a stock solution (0.1%) dissolving 0.1 g of N-1-naphthylethylenediamine dihydrochloride in 100 mL of deionized water (Elga, UK). Then in a volumetric flask of 1 L, we added 600 mL of deionized water and 140 mL of glacial acetic acid, dissolved 5 g of sulphanilic acid, added 20 mL of the indicated stock solution (0.1%) of N-1-naphthylethylenediamine dihydrochloride, and finally diluted to 1 L.

Standard solutions were prepared using solutions of NaNO<sub>2</sub> and the concentration was converted into equivalent [NO<sub>2</sub>]. In his seminal work, Salzmann empirically observed that 0.72 moles of NaNO<sub>2</sub> produced the same colour as 1 mole of NO<sub>2</sub>. 15 However, more recent investigations have found that such conversion factor is closer to 0.82.34,35 As we prepared a stock of solution of 20.3 ppm of NaNO2, it contains the equivalent of  $[NO_2] = 16.5$  ppm calculated using the formula:

[NO<sub>2</sub>] (ppm) = 
$$\frac{C_{\text{NaNO}_2}^{\text{ppm}}}{\text{MW}_{\text{NaNO}_2}} \times \frac{\text{MW}_{\text{NO}_2}}{0.82}$$
 (1)

Calibration solutions of 0.1, 0.2, 0.4, 0.6, 0.8, and 1 ppm equivalent [NO<sub>2</sub>] were prepared using appropriate amounts of NaNO<sub>2</sub> and diluting with the absorbing solution allowing 15 min for full colour development.

In addition, a series of mock samples containing the equivalent of 0.05, 0.15, 0.3, and 0.5 ppm of NO<sub>2</sub> were also prepared using the same procedure.

#### In situ sampler/analyser

The sampling train consisted of a 4.5 V air pump (RS PRO Series D250, RS Components, Corby, UK; £50), a rotameter (MR rotary series, model 3A13, Key Instruments, Trevose, PA, USA; £80), and an impinger (Supelco, Bellefonte, PA, USA; £70) which was used to trap the NO2 using an absorbing reagent. Colour analysis was performed using an 8 MP camera (Raspberry Pi Camera V2, Cambridge, UK; £15), connected to a Raspberry Pi computer (Model 3B+, Cambridge, UK; £60). A simple white USB LED light (YLC; £1) was connected to the Raspberry Pi and used to maintain a constant light intensity (we do not need a specific wavelength but to keep it constant in relation to the calibration). All components were placed in a light- and weather-proof box (Luceco PLC, London, UK; £15). The box had some watertight overtures on one side through which tubing can pass for air sampling and power supply. The prices of the main elements of the sampling train are given as an indicator and amount to

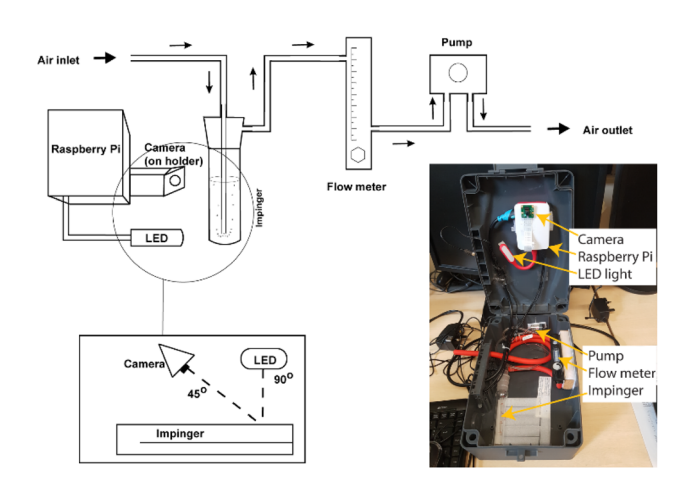


Fig. 1 PiSENS-A: schematic representation of the sampling train and an image of the device.

£291. Note that the prices are correct on the date of purchase (during 2022) and are subject to change.

#### Accessories

SketchUP (Trimble, Sunnyvale, CA, USA) was used for designing accessories printed on the 3D printer (Ultimaker 2+, Ultimaker D.V. Utrecht, the Netherlands). In particular, we created a camera holder with a triangular shape to position the camera with an inclination of 45° in relation to the impinger, while the LED light was at 90° directly on top (Fig. 1). We also created a Raspberry Pi holder for keeping the camera and computing system adjacent to the impinger, but not obstructing it. This allows for easy replacement of the absorbing reagent and standard solutions. The PiSENS-A is illustrated in Fig. 1. The inset image illustrates the device, but please note that the camera, Raspberry Pi, and the LED light are separated from their operating position for the purpose of clarity.

#### Validation in the laboratory

For characterization and calibration purposes spectrophotometric analyses were performed using a Varian Cary 50 UV-vis Spectrophotometer (Mulgrave, Australia).

#### Calculations

Statistical calculations were performed with MS Excel software (Microsoft Co, Redmond, WA, USA). The Raspberry Pi computing system used Raspbian OS (Raspberry Pi Foundation, Cambridge, UK). The determination of colour intensity and calculation of [NO<sub>2</sub>] was performed using in-house written code in Python programming language (PSF, Wilmington, Delaware, USA).

To compute [NO<sub>2</sub>] in air analysed over a specific period of time (e.g. 1 h for the determination of hourly mean, or 24 h for daily mean), one needs to consider several details.

It is also important to define some terminology here. Traditionally, devices using Griess-Saltzman (GS) reaction sample air and are thus called samplers', while the analysis is done in the lab. PiSENS-A on the other hand samples the air and is doing the analysis (imaging of colour of the absorbing solution and its automatic conversion into concentration) instantaneously using python script. Thus we will refer to the entire process as 'analysis' rather than 'sampling'.

**Equivalent** [NO<sub>2</sub>]. The script written in Python programming language is capable of conversion of 'projections' (for the explanation of this term, please refer to the section Theory) into concentration in ppm. Given that standard solutions are prepared using NaNO<sub>2</sub>, it is essential to convert its concentration into equivalent [NO<sub>2</sub>] as explained above, using eqn (1). Note that only one conversion is necessary, *i.e.* either for the concentration of standard solutions, or the PiSENS-A's calculated concentrations. We refer to this concentration as [NO<sub>2</sub>]-corr Pisens-A and is calculated using eqn (1).

**Evaporation of absorption solution.** The loss of absorbing solution may present as a significant issue, especially during longer analysis times and/or temperature variations. The simplest solution is to measure the volume of the absorbing solution before and after the end of the analysis period. We ran numerous experiments using different initial volumes (10 and 15 mL) and different duration times (24, and 72 hours). The results of the evaporation rate were very similar in all cases with an average rate of 0.138  $\pm$  0.01 mL h $^{-1}$ . We use this value to calculate the corrected volume of absorption solution as:

$$V_{\text{abs.sol}}^{\text{corr}} = V_{\text{abs.sol}}^{\text{start}} - r_{\text{evap}} \times t_{\text{analysis}}$$
 (2)

where  $V_{\rm abs.sol}^{\rm start}$  is the volume of absorbing solution at the beginning,  $r_{\rm evap}$  is the rate of evaporation and  $t_{\rm analysis}$  is the analysis time.

The volume of analysed air. It is important to consider atmospheric conditions in order to obtain accurate values for the volume of air analysed for a given period of time ( $V_{air}^t$ ). We obtained this using the following equation:

$$V_{\text{air}}^{t,\text{corr}} = V_{\text{air}}^{t} \times \frac{P}{P_{\text{SATP}}} \times \frac{T_{\text{SATP}}}{T}$$
 (3)

where  $V_{\rm air}{}^t$  is obtained experimentally considering the air flow rate (Q) and the time of analysis as  $V_{\rm air}{}^t = Q \times t_{\rm analysis}$ .  $P_{\rm SATP}$  and  $T_{\rm SATP}$  are Standard Ambient Temperature and Pressure (SATP) defined as 101 325 Pa and 298.15 K respectively, while P and T are atmospheric pressure and temperature.

To compute the concentration of  $NO_2$  in the air for a specific period, the following formula was applied:

$$[NO_{2}]_{AIR} \ (\mu g \ m^{-3}) = \ \frac{\left([NO_{2}]_{PiSENS-A}{}^{t,corr} - [NO_{2}]_{PiSENS-A}{}^{t=0,corr}\right) \ (mg \ L^{-1}) \times 1000 \ \mu g \ mg^{-1} \times V_{abs.sol.}^{corr} \ (L)}{\left(V_{air}{}^{t,corr} - V_{air}{}^{t=0,corr}\right) \ (L) \times 0.001 \ m^{3} \ L^{-1}} \ (4)$$

where  $[NO_2]_{PiSENS-A}^{t=0,corr}$  and  $V_{air}^{t=0,corr}$  signify the corrected [NO<sub>2</sub>] and volume of analysed air respectively at the beginning of a given analysis period which does not necessarily coincide with the global start of the analysis. Since the GS reaction is cumulative, in a 24 h-long analysis, we could calculate 24 hourly means each beginning at the end of the previous measuring period.

#### Griess-Saltzman reaction characterization

The Griess-Saltzman reaction has been largely used and tested since it was first published in 1954. In the late 1960s, Pratt and Whitney used this method for measuring NO<sub>2</sub> in engine exhaust gasses studying the sensitivity, the effects of other contaminants, and the time-temperature effect on stored developed solutions.36 For example, it was found that SO2 and O3 present the most significant interferences. The former may cause an error of up to 7.5% if present in concentrations of >15 ppm. Fortunately, such concentrations are not found anymore in modern car engines. Ozone may cause a small interference if present in a five-fold ratio to NO2, causing the maximum effect at  $\sim$ 3 h after the end of sampling. 35,36 Similar results about these pollutants have been reported in more recent studies (e.g. Passaretti Filho et al.).30 Under the conditions in which PiSENS-A is tested, it would be extremely rare to find concentrations of SO<sub>2</sub> and O<sub>3</sub> that could interfere with the measurements of NO<sub>2</sub>. Other potential interferences present in the air such as humidity, methane, carbon monoxide or ammonia produce no significant effects on Griess-Saltzman (GS) reaction-based methods.28

Furthermore, the literature suggests that it takes about 15 min for the colour to develop, the method should not be used for longer than 60 min in an atmosphere with extremely high levels of NO2 (~20 ppm) due to the potential saturation of absorbing solution, the optimum air flow rate is between 0.2 and 0.4 L min<sup>-1</sup>, and that this method can be used with a NO<sub>2</sub> concentration range in the air that goes from 0.002 to 5 ppm.<sup>29,30,35</sup> Since expected levels of NO<sub>2</sub> in the air in which we tested PiSENS-A are well within these values, we were confident in our ability to sample for longer periods (up to 72 h).

#### Validation and evaluation in the field

The PiSENS-A has been validated and evaluated using four experimental arrangements.

Discrete sampling/analysis. The PiSENS-A was placed about 50 cm from the exhaust pipe of an idling car while the air was analysed for specific time intervals (e.g. 15, 30, 45 minutes) at 0.35 L min<sup>-1</sup>. The calibration of the PiSENS-A was performed in situ prior to starting the engine. This arrangement mimicked the traditional setup where the air is sampled during discrete time intervals followed by the analysis in lab-controlled conditions as was suggested in the original work by Saltzman. 15

Continuous in situ analysis. The PiSENS-A was placed about 50 cm from the exhaust pipe of an idling car but this time, the analysis was carried out in intervals of five minutes over a period of up to 1 h. Moreover, a blank experiment was

performed under the same conditions but in a garden area away from the car and any road traffic.

In both discrete and continuous analysis, all measurements were performed in duplicate.

Continuous in situ analysis next to an air quality monitoring station. In order to validate PiSENS-A against a traditional methodology for continuous analysis, we placed PiSENS-A at  $\sim$ 5 m from the DEFRA's monitoring station (UK identification code UKA00337). The station utilizes a chemiluminescence-based methodology. It belongs to DEFRA Automatic Urban and Rural Monitoring Network (AURN) and is operated by Bureau Veritas. The station is located in Stoke-on-Trent, UK, adjacent to a busy shopping centre (location coordinates: easting/northing: 388 351, 347 895). Analysis was carried out on three different days.

Long-term, continuous in situ analysis. Following the extensive validation as explained above, we deployed PiSENS-A in the garden area of the Crime Scene House (CSH) at Keele University which is located at one of the main roads on the campus and adjacent to a bus stop. The analysis was carried out every minute over a period of 24 h and repeated for two days.

In all four arrangements, we also collected all the ancillary data needed to calculate the concentration of NO2 in the air using eqn (4) as explained in the section 'Calculations'.

# Theory

Digital colourimetry uses several different colour systems for quantitative assessment of colour. One of the most commonly used systems is referred to as RGB and refers to the intensities of separate red, green, and blue light sources that can be mixed to create a different colour. The RGB system is the standard method of representing colour images on screens, such as TVs, computer monitors, and smartphone screens. The possibilities for mixing the three colours together can be represented as a threedimensional coordinate system with the values for R (red), G (green) and B (blue) on each axis. This coordinate system yields a cube called the RGB colour space as represented in Fig. 2 left.

If all three colour channels have a value of zero, it means that no light is emitted and the resulting colour is black (on a monitor, for example, it cannot be blacker than the surface of the monitor producing zero light). If all three colour channels are set to their maximum values (typically 255 for complete light saturation in an 8 bit representation where  $2^8 = 256$ ), the resulting colour is white. This type of colour mixing is also called "additive colour mixing".

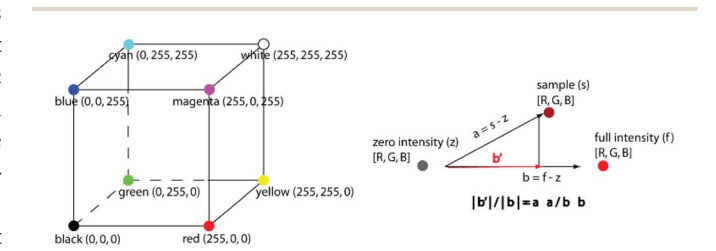


Fig. 2 (Left) RGB space. (Right) Representation of a sample vector s and its projection onto one of the coordinates (b') along with its scalar value.

For any chemical system where colour is dependent on concentration, it should be possible to process a digital image of the sample to obtain an estimate of concentration. If only 1 of the 3 RGB colour channels is significantly dependent on concentration, a simple approach would look only at this channel and disregard the other two. However, it is often the case that the concentration affects all 3 channels to a certain extent, so a more accurate measurement would use the intensity of all 3.

The approach taken here maps the 3-tuple RGB position, *i.e.* the coordinate with the 3 values that correspond to R, G, and B respectively, to a scalar value by calculating the scalar projection of a sample RGB 'vector' on a base 'vector' representing the overall min/max range (Fig. 2 right). Note that the term 'vector' is convenient to use although the RGB space is obviously not an actual vector space. The base vector, b, is the [R, G, B] tuple of the highest concentration (max) sample minus the [R, G, B] tuple of the zero (min) concentration sample (*i.e.*  $R_{max} - R_0$ ,  $G_{max} - G_0$ ,  $G_{max} - G_0$ ,  $G_{max} - G_0$ ,  $G_{max} - G_0$ ). The sample vector, a, is the [R, G, B] tuple of the sample being measured minus the [R, G, B] tuple of the zero (min) concentration sample.

The scalar value of the length of the projection b' of a onto b is given by  $\frac{a \cdot b}{|b|}$  (where  $\cdot$  is the dot product operator) and as  $\frac{a \cdot b}{b \cdot b}$  as a ratio to the length of b.

Using a series of samples of known concentration across the range of interest, a plot of projection values against concentration values (or a function of concentration values) provides a calibration curve which can then be used to estimate the concentration of unknown samples within this range. This simple approach makes no attempt to relate the RGB intensity values to concentration using physical interpretations (*e.g.* Beer–Lambert law *etc.*) – something which would require a significant understanding of the specific inner workings of the camera device itself and would therefore not be without difficulty. For more information on the rationale and approach to calibration, please read section 'Background' in the ESI.†

To automate the analysis and simplify the usage, we have written a python script which utilizes the principles outlined above. The script can be found in the ESI† section 'Python script'.

We chose to use the piecewise cubic Hermite interpolating polynomial (pchip) implemented within the SciPy library (scipy.interpolate.pchip) to generate a reasonably smooth curve. It has been shown that the use of the approach showed robust and efficient performance.<sup>37–39</sup> The code could fairly easily be modified to fit the calibration points to any arbitrary curve using, for instance, scipy.optimize.

Fig. 3 shows the calibration by PiSENS-A. As noted above, there is no expectation of linearity since there is no relationship between RGB intensity values and the Beer–Lambert law. Please remember that significant curvature of the projection of the calibration function curve onto the base vector is allowed as long as it is monotonic (see ESI, section 'Background'†). In other words, as the shade of purple colour of  $[NO_2]$  calibration solutions darkens, its RGB components change inducing variations in projections onto the base vector which does not have to be linear.

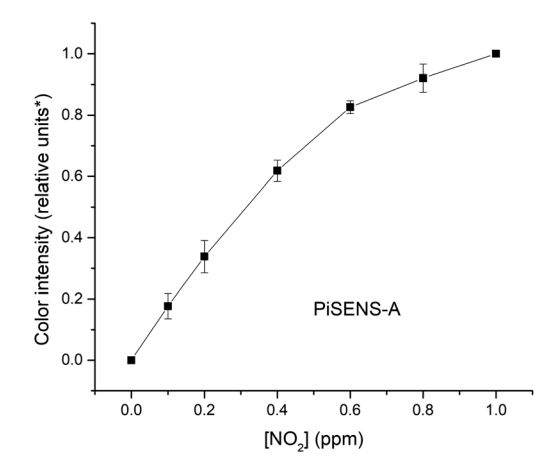


Fig. 3 Calibration of PiSENS-A using equivalent  $[NO_2]$  standards using eqn (1). Error bars are standard deviations of four tests. \*A proportional scalar projection of (sample [RGB] — zero [RGB]) onto (max [RGB] — zero [RGB]).

#### Results and discussion

#### Pre-calibration of PiSENS-A using variable shades

In order to test the reliability of the algorithm and to evaluate light conditions (illumination intensity, and position and distance of light source) and position of the camera in relation to impinger and other elements within PiSENS-A, numerous pre-calibration tests were carried out. Initially, sets of 10 increasingly stronger shades of orange, green, pink and blue paper were used. A white paper was used as a reference (zero intensity) while the maximum intensity (1) was set using the darkest shade. The measured colour intensities across the range of shades were monotonic. The average of 10 subsequent measurements of colour intensity for each shade, plotted against the initial colour intensity measurement for each shade produced a linear relationship with an  $R^2$  value of 0.9986, 0.9937, 0.9994, and 0.9987 for the orange, green, pink and blue series respectively, indicating that the colour measurement was consistent and repeatable across these ranges (please see ESI, section 'Pre-calibration with reference papers', Fig. SI3-SI5†). Initial tests indicated that optimal results are obtained when the sampling area was fixed inside the box at the same position maintaining the same interior light conditions. The light was located at the angle of 90° to the sampling area at a distance of approximately 5 cm. The imaging camera was located at a distance of approximately 10 cm at an angle of 45° as was suggested by Johnsen.40

#### Analytical characterization of PiSENS-A

In this study, we decided to test PiSENS-A for potential application in air quality analysis by *in situ* monitoring of  $[NO_2]$  in air. Calibration of the PiSENS-A system was performed by placing 10 mL of calibration solution into the impinger and closing the lid while maintaining the previously determined optimal light and position conditions. The non-exposed absorbing solution was used as a blank (dedicated as  $[NO_2]$  =

0 ppm). Several different concentrations across the desired range of measurement were analysed and a calibration curve was generated from the measured colour intensities. To provide a workable range of measurement, the highest calibration concentration was chosen to be well above the highest likely sample concentration.

A set of 7 standard solutions between 0-1 ppm (e.g. 0, 0.1, 0.2, 0.4, 0.6, 0.8 and 1.0 ppm of equivalent [NO<sub>2</sub>]) were used in the calibration. All measurements were done in triplicate, and four tests were carried out to evaluate the reproducibility of the calibration curve (Fig. 3).

Under the operating conditions (10 mL of absorbing solution and airflow rate  $Q = 0.35 \text{ L min}^{-1}$ ) this range corresponds to hourly  $[NO_2] = 0 \mu g m^{-3} - [NO_2] = 476 \mu g m^{-3}$  respectively which is within the range of the lowest DEFRA's Air Quality Index<sup>41</sup> having a maximum of  $[NO_2] = 67 \mu g m^{-3}$ . For further evaluation purposes, the same set of calibration solutions was recorded using a laboratory UV-vis instrument (Fig. SI6 in ESI, section 'Calibration with [NO<sub>2</sub>] standards'†). The LOD as S/N = 3 was determined by recording a separate blank solution and obtained LOD =  $7.14 \times 10^{-5}$  ppm equivalent [NO<sub>2</sub>] corresponding to hourly  $[NO_2] = 0.034 \, \mu g \, m^{-3}$ .

Following the calibration, we prepared four mock samples which were analysed using both PiSENS-A and laboratory UV-vis spectrophotometer for comparison. These four mock samples were analysed in three independent sets (N = 3). The results are presented in Table 1 while Fig. 4 demonstrates the correlation between results obtained by the two instruments. The accuracy obtained by PiSENS-A (RE% = 6.64%) is better than those reported in the literature by Passaretti Filho et al. in 2019 (RE% =  $(12\%)^{32}$  and in 2015 for high NO<sub>2</sub> (>15 ppb; RE% = 7%), obsta worse than that in 2015 for low NO<sub>2</sub> (<54 ppb; RE% = 2%).<sup>30</sup> It is noteworthy that the precision of PiSENS-A (RSD% = 2.85%) is comparable to the ones from recently reported similar devices e.g. portable active samplers reported by Subba et al. (RSD% = 3.6%),42 Tian et al. (RSD% = 4.1%),31 Cerrato-Alvarez et al. (RSD% = 9%),  $^{29}$  passive samplers developed by Felix et al. (3.4 < RSD% > 7.2%),43 or passive microsamplers developed by Passaretti Filho et al. (RSD% = 6.9%). Further comparisons of analytical characteristics between several relevant methods and PiSENS-A are given in ESI Table SI1.†

Table 1 Averaged precision and accuracy of the NO<sub>2</sub> measurements expressed as relative standard deviation (RSD%) and per cent relative error (RE%) obtained for four different mock samples from three different independent tests (N = 3) by PiSENS-A and the lab-based UVvis spectrophotometer

	PiSENS-A			UV-vis			
[NO <sub>2</sub> ] (ppm)	$\begin{array}{c} \text{Mean} \pm \\ \text{SD} \end{array}$	RSD%	RE%	$\begin{array}{c} \text{Mean} \ \pm \\ \text{SD} \end{array}$	RSD%	RE%	
0.05	$0.055 \pm 0.002$	F 21	0.57	$0.044 \pm 0.003$	F 02	10.64	
0.05	$0.055 \pm 0.002$	5.31	9.57	$0.044 \pm 0.003$	5.03	12.64	
0.15	$0.16\pm0.01$	4.08	6.51	$0.152 \pm 0.003$	2.34	1.52	
0.3	$0.31\pm0.02$	1.03	6.92	$\textbf{0.299} \pm \textbf{0.006}$	1.39	0.26	
0.5	$0.51\pm0.02$	1.01	3.56	$\textbf{0.499} \pm \textbf{0.002}$	1.44	0.14	

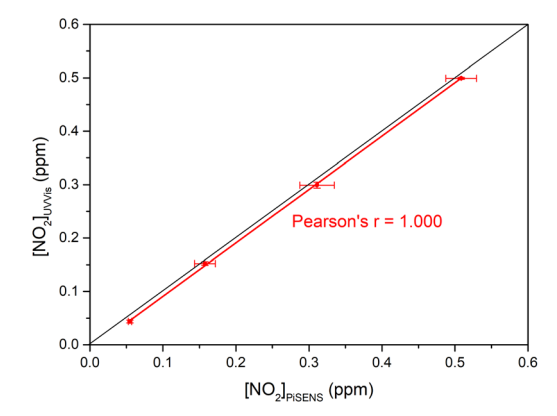


Fig. 4 Correlation of results (SE n = 3) for mock samples (target [NO<sub>2</sub>] = 0.05, 0.15, 0.30, and 0.50 ppm) obtained by PiSENS-A and UV-vis.

#### Continuous monitoring of [NO<sub>2</sub>] in the air

Encouraged by the excellent correlation of results obtained by PiSENS and laboratory UV-vis, we carried out further tests outdoors. Initial tests involved placing the PiSENS-A next to an idling car's exhaust pipe as explained in the 'Field experiment' section of the Experimental. We rationalized that this arrangement would simulate heavy traffic conditions during, for example, rush hour. Thus we could demonstrate the ability of PiSENS-A to continuously monitor [NO2] in the air with significant improvement in temporal resolution relative to other wet chemistry methods, 15,44 and passive samplers. 45 On the other hand, low costs yet robust PiSENS-A system offers an opportunity to significantly reduce the cost relative to chemiluminescence as the current reference methodology for obtaining hourly [NO2]46 or allow the operations under unfavourable weather conditions that limit the performance of differential optical absorption spectroscopy (DOAS).47 Exploiting the ability of PiSENS-A to perform analysis at almost any time interval, we decided to perform analysis in small time increments (5 minutes) in duplicate over the period of 1 hour since hourly mean is considered an important parameter of ambient air quality analysis. For example, DEFRA's Air Quality Strategy states that 200 μg m<sup>-3</sup> as an hourly mean should not be exceeded more than 18 times per vear.27

The control experiment was performed by placing the PiSENS-A in a garden area which has minimal exposure to road traffic using the same analysis pattern. For illustration purposes, Fig. 5 shows the evolution of the colour signal obtained as a consequence of exposure to the constant source of NO2 (black) and the control (red). This is to clearly demonstrate the colour instability in the initial  $\sim$ 20 min of analysis as discussed in the section 'Griess-Saltzman reaction characterization'. While it is possible to present [NO<sub>2</sub>] calculated per minute or even shorter sampling times, we found that such data presentation may be confusing and misleading. Obtained total hourly [NO2] at the source was [NO2]  $_{source}$  = (98  $\pm$  1)  $\mu g\,m^{-3}$  with the control  $[NO_2]_{control} = (29 \pm 1) \,\mu g \, m^{-3}$ .

To validate PiSENS-A for long-term monitoring against a traditional methodology, three sampling campaigns were

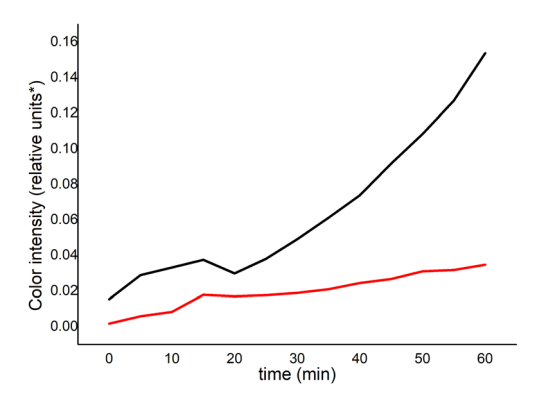


Fig. 5 Monitoring of  $[NO_2]$  in the air. The signal (colour intensity as measured by the Raspberry Pi) as a function of sampling time, when the PiSENS-A was placed adjacent to the exhaust pipe in black, and when the PiSENS-A was placed in the garden area in red. \*A proportional scalar projection of (sample [RGB] - zero [RGB]) onto (max [RGB] - zero [RGB]), please see ESI.†

**Table 2** Comparative measurements of  $[NO_2]$  using PiSENS-A and DEFRA's monitoring station using the chemiluminescent method (AURN – DEFRA monitoring station at Hanley, Stoke on Trent). DEFRA's data are publicly available while we enclose data for July 2022 in the ESI as a separate MS Excel file

Sampling time/day	$[NO_2]$ PISENS	[NO <sub>2</sub> ] DEFRA	Dif	RE%
17:30–19:00 July 11th 2022	18.3	18.7	-0.4 $0.2$ $-0.3$	2.1
19:05–20:35 July 16th 2022	22.2	21.9		1.4
17:25–18:55 July 18th 2022	21.5	21.8		1.4

carried out next to a DEFRA's monitoring station as described in the section 'Field experiment'. Considering the initial colour instabilities, we decided to analyse for 90 min and determine the hourly mean for the last 60 min of analysis. Table 2 shows excellent agreement between data obtained by PiSENS-A and the monitoring station (Pearson r=0.993). It is interesting to note that these field tests took place during a heat wave when the temperature reached a highly unusual 33 °C. Given that some of the tests were performed during December 2021 with ambient temperatures of 5–10 °C, these results not only demonstrate the accuracy and precision of PiSENS-A, but its ability to work under very different weather conditions.

Satisfied with PiSENS-A's performance validation, we decided to deploy it in a fully independent field trial. We chose Keele's CSH as a location that offers exposure to a relatively busy road, convenient access and protection of and from the public. Fig. 6 exhibits data obtained for monitoring of  $[NO_2]$  over 24 h on two different days. Note that the relatively low  $[NO_2]$  is easily explained by the geography of the Keele campus. The buildings are spread over a wide area surrounded by plenty of trees and green areas. The entire campus is located on a small, windy hill in the vicinity of Keele village which is approximately 5 km from the closest town of Newcastle-under-Lyme, and approximately 8 km from the city centre of the busy, commercial city of Stoke-on-Trent, UK. For comparison purposes, we show  $[NO_2]$  obtained at

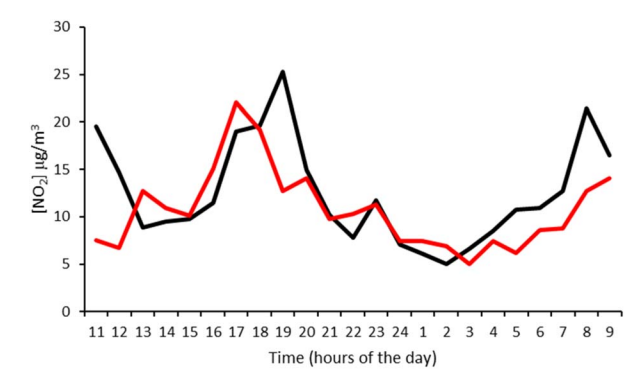


Fig. 6 Determination of hourly  $[NO_2]$  in the air at the Crime Scene House at the Keele University campus. (Black) The hourly  $[NO_2]$  in the air analysed from 10 am 03rd-9 am 04th Wednesday to Thursday. (Red) The hourly  $[NO_2]$  in the air monitored from 10 am 05th-9 am 06th Friday to Saturday.

CSH-Keele and by DEFRA's AURN in Stoke-on-Trent at the city centre (Hanley) and at the roadside (A50) in Fig. SI7.† Briefly, as expected, the results from the busy roadside are significantly higher than at the Keele campus (Fig. SI7†).

Despite low measured  $[NO_2]$ , we observe that PiSENS-A is capable of capturing interesting temporal changes (Fig. 6). This is for example illustrated by an increase of  $[NO_2]$  in the afternoon most likely coinciding with people leaving the campus for the day. Also, as expected, the overnight  $[NO_2]$  is very similar on both days as there are no fresh fluxes of  $NO_2$ . It can also be observed that the measured  $[NO_2]$  in morning hours, possibly originating from the increase in activity and traffic, is higher on a working day than on Saturday.

The presented results demonstrate that PiSENS-A can be successfully used for the continuous NO2 monitoring of air quality for 24 hours. We are confident that the duration of analysis can be extended even further (48 h or maybe even 72 h). We base this confidence on two factors: (a) the span of the calibration curve (max of  $[NO_2]_{AIR} = 1191 \mu g m^{-3}$  using the maximum capacity of absorbing solution) which covers the highest measured values of hourly concentrations of NO2 as well as the average cumulative for 48 h obtained at Stoke-on-Trent's measuring station for the period of June 2021-June 2022 (129 μg m<sup>-3</sup> and 913 μg m<sup>-3</sup> respectively). 48 In addition, this calibration range would cover the entire scale of DEFRA's Air Quality Index scale for hourly concentrations of NO<sub>2</sub> spanning  $0 \mu g m^{-3} < [NO_2] < 601 \mu g m^{-3}$  (corresponding to indexes 1 and 10 respectively).41 (b) Importantly, our confidence is based on a design of PiSENS-A that contains two impingers thus doubling the capacity of analysis. We have run preliminary experiments with two impingers for 72 hours and obtained promising data (not shown). Since such a design requires further testing and optimising, the data will be reported in the future.

#### Conclusions

We developed a computer-vision-based device that facilitates digital colourimetry which we refer to as PiSENS. Herein we demonstrated its functionality for monitoring  $[NO_2]$  in the air

Paper

Published on 22 December 2022. Downloaded by Tufts University on 2/1/2024 5:27:17 PM.

and thus we refer to it as PiSENS-A. It was constructed using low-cost materials that can be found in DIY shops and/or be 3D printed. The low-cost computer (Raspberry Pi) with its digital camera is PiSENS-A's sensing core. A simple code written in Python allows continuous imaging and analysis of the colour developed, for example, as a consequence of a chemical reaction. In this example, we utilize the traditional Saltzman reaction for the detection of NO<sub>2</sub> where the colour is developed in the reaction of NO2 with the solution of N-1-naphthylethylenediamine dihydrochloride used as an absorber. As a fully functional device, PiSENS-A is accurate (RE% = 6.64%), precise (RSD% = 2.85%), fully portable, and inexpensive. In addition, PiSENS provides a wide linear range, an excellent detection limit of 0.034 μg m<sup>-3</sup> and reproducibility. Moreover, it was validated in an urban environment against a governmentregulated monitoring station (Pearson r = 0.993) and deployed as an independent station for monitoring air quality at the Keele campus.

With the low construction and operational cost, as well as the ability to continuously monitor the analyte of choice (in this case [NO2]) over very short times, PiSENS-A shows the potential to significantly improve the spatio-temporal frequency of analysis. Furthermore, the WiFi and/or Bluetooth capability of Raspberry Pi might also be exploited for instantaneous data transmission, mapping, and the development of large-scale networks assisting in the development of high-precision models. In the case of air quality analysis, we envision a possibility for deployment in rural and/or remote communities where the placement of fixed, expensive and complex instruments that are currently being used is very limited.

#### Conflicts of interest

The authors declare no competing financial interests.

# Acknowledgements

This work has been generously supported by British Council (413876777) and NSF-UKRI (NE/T012331/1). IB gratefully acknowledges support from ERASMUS+ K107 ICM (2019-1-UK01-KA107-061362). S. E. T. and G. P. are grateful to FONDECYT-BC (grant #227-2018-FONDECYT). The authors are also thankful to DEFRA for provision of data for [NOx] from Stoke-on-Trent Centre location of AURN (© Crown 2021 copyright Defra via https://uk-air.defra.gov.uk, licenced under the Government Licence (https:// Open www.nationalarchives.gov.uk/doc/open-government-licence/ version/2/) (OGL)).

#### References

- 1 S. K. Vashist, P. B. Luppa, L. Y. Yeo, A. Ozcan and J. H. T. Luong, Emerging Technologies for Next-Generation Point-of-Care Testing, Trends Biotechnol., 2015, 33(11), 692-705, DOI: 10.1016/j.tibtech.2015.09.001.
- 2 J. G. E. Gardeniers and A. van den Berg, Lab-on-a-Chip Systems for Biomedical and Environmental Monitoring,

- Anal. Bioanal. Chem., 2004, 378(7), 1700-1703, DOI: 10.1007/s00216-003-2435-7.
- 3 D. Diamond, S. Coyle, S. Scarmagnani and J. Hayes, Wireless Sensor Networks and Chemo-/Biosensing, Chem. Rev., 2008, 108(2), 652-679, DOI: 10.1021/cr0681187.
- 4 G. Matzeu, L. Florea and D. Diamond, Advances in Wearable Chemical Sensor Design for Monitoring Biological Fluids, Sens. Actuators, B, 2015, 211, 403-418, DOI: 10.1016/ j.snb.2015.01.077.
- 5 A. Ozcan, Mobile Phones Democratize and Cultivate Next-Generation Imaging, Diagnostics and Measurement Tools, 2014, **14**(17), 3187–3194, DOI: **10.1039**/ Chip,C4LC00010B.
- 6 A. P. Dhawan, W. J. Heetderks, M. Pavel, S. Acharya, M. Akay, A. Mairal, B. Wheeler, C. C. Dacso, T. Sunder, N. Lovell, M. Gerber, M. Shah, S. G. Senthilvel, M. D. Wang and B. Bhargava, Current and Future Challenges in Point-of-Care Technologies: A Paradigm-Shift in Affordable Global Healthcare With Personalized and Preventive Medicine, IEEE Journal of Translational Engineering in Health and Medicine, 2015, 3, 1-10, DOI: 10.1109/JTEHM.2015.2400919.
- 7 Teach, Learn, and Make with Raspberry Pi Raspberry Pi, https://www.raspberrypi.org/, accessed 2020-07-19.
- 8 M. O'Brien, L. Konings, M. Martin and J. Heap, Harnessing Open-Source Technology for Low-Cost Automation in Synthesis: Flow Chemical Deprotection of Silyl Ethers Using a Homemade Autosampling System, Tetrahedron Lett., 2017, 58(25), 2409-2413, DOI: 10.1016/ j.tetlet.2017.05.008.
- 9 M. O'Brien, A. Hall, J. Schrauwen and J. van der Made, An Open-Source Approach to Automation in Organic Synthesis: The Flow Chemical Formation of Benzamides Using an Inline Liquid-Liquid Extraction System and a Homemade 3-Axis Autosampling/Product-Collection Device, Tetrahedron, 2018, 74(25), 3152-3157, DOI: 10.1016/ j.tet.2018.02.043.
- 10 G. S. Luka, E. Nowak, J. Kawchuk, M. Hoorfar and H. Najjaran, Portable Device for the Detection of Colorimetric Assays, R. Soc. Open Sci., 2017, 4(11), 171025, DOI: 10.1098/rsos.171025.
- 11 Air Pollution, https://www.who.int/westernpacific/healthtopics/air-pollution, accessed 2021-07-14.
- 12 Air Pollution: Coroner Calls for Law Change after Ella Adoo-Kissi-Debrah's Death, BBC News, 2021.
- 13 Y. Y. Maruo, S. Ogawa, T. Ichino, N. Murao and M. Uchiyama, Measurement of Local Variations in Atmospheric Nitrogen Dioxide Levels in Sapporo, Japan, Using a New Method with High Spatial and High Temporal Resolution, Atmos. Environ., 2003, 37(8), 1065-1074, DOI: 10.1016/S1352-2310(02)00974-3.
- 14 Q. Di, H. Amini, L. Shi, I. Kloog, R. Silvern, J. Kelly, M. B. Sabath, C. Choirat, P. Koutrakis, A. Lyapustin, Y. Wang, L. J. Mickley and J. Schwartz, Assessing NO 2 Concentration and Model Uncertainty with High Spatiotemporal Resolution across the Contiguous United States Using Ensemble Model Averaging, Environ. Sci.

- Technol., 2020, 54(3), 1372–1384, DOI: 10.1021/acs.est.9b03358.
- 15 B. E. Saltzman, Colorimetric Microdetermination of Nitrogen Dioxide in Atmosphere, *Anal. Chem.*, 1954, **26**(12), 1949–1955, DOI: **10.1021/ac60096a025**.
- 16 B. Krupińska, A. Worobiec, G. Gatto Rotondo, V. Novaković, V. Kontozova, C.-U. Ro, R. Van Grieken and K. De Wael, Assessment of the Air Quality (NO2, SO2, O3 and Particulate Matter) in the Plantin-Moretus Museum/Print Room in Antwerp, Belgium, in Different Seasons of the Year, *Microchem. J.*, 2012, 102, 49–53, DOI: 10.1016/j.microc.2011.11.008.
- 17 Y. Wang, A. Allen, D. Mark and R. M. Harrison, Development of a Personal Monitoring Method for Nitrogen Dioxide and Sulfur Dioxide with Sep-Pak C18 Cartridge Sampling and Ion Chromatographic Determination, *J. Environ. Monit.*, 1999, 1(5), 423–426, DOI: 10.1039/a905305k.
- 18 A. A. Salem, A. A. Soliman and I. A. El-Haty, Determination of Nitrogen Dioxide, Sulfur Dioxide, Ozone, and Ammonia in Ambient Air Using the Passive Sampling Method Associated with Ion Chromatographic and Potentiometric Analyses, Air Qual., Atmos. Health, 2009, 2(3), 133–145, DOI: 10.1007/s11869-009-0040-4.
- 19 Y. Yan, J. Sun, K. Zhang, H. Zhu, H. Yu, M. Sun, D. Huang and S. Wang, Visualizing Gaseous Nitrogen Dioxide by Ratiometric Fluorescence of Carbon Nanodots-Quantum Dots Hybrid, *Anal. Chem.*, 2015, **87**(4), 2087–2093, DOI: **10.1021**/ac503474x.
- 20 Y. Yan, S. Krishnakumar, H. Yu, S. Ramishetti, L.-W. Deng, S. Wang, L. Huang and D. Huang, Nickel(II) Dithiocarbamate Complexes Containing Sulforhodamine B as Fluorescent Probes for Selective Detection of Nitrogen Dioxide, *J. Am. Chem. Soc.*, 2013, 135(14), 5312–5315, DOI: 10.1021/ja401555y.
- 21 K. Li, Y. Zhao, X. Yuan, H. Zhao, Z. Wang, S. Li and S. S. Malhi, Comparison of Factors Affecting Soil Nitrate Nitrogen and Ammonium Nitrogen Extraction, *Commun. Soil Sci. Plant Anal.*, 2012, 43(3), 571–588, DOI: 10.1080/ 00103624.2012.639108.
- 22 C. Lin, J. Gillespie, M. D. Schuder, W. Duberstein, I. J. Beverland and M. R. Heal, Evaluation and Calibration of Aeroqual Series 500 Portable Gas Sensors for Accurate Measurement of Ambient Ozone and Nitrogen Dioxide, *Atmos. Environ.*, 2015, 100, 111–116, DOI: 10.1016/j.atmosenv.2014.11.002.
- 23 M. Hossain, J. Saffell and R. Baron, Differentiating NO<sub>2</sub> and O<sub>3</sub> at Low Cost Air Quality Amperometric Gas Sensors, ACS Sens., 2016, 1(11), 1291–1294, DOI: 10.1021/acssensors.6b00603.
- 24 G. F. Fine, L. M. Cavanagh, A. Afonja and R. Binions, Metal Oxide Semi-Conductor Gas Sensors in Environmental Monitoring, *Sensors*, 2010, **10**(6), 5469–5502, DOI: **10.3390**/ **\$100605469**.
- 25 Y. Sun, L. Wang, Y. Wang, L. Quan and L. Zirui, In Situ Measurements of SO2, NOx, NOy, and O3 in Beijing, China during August 2008, *Sci. Total Environ.*, 2011, 409(5), 933–940, DOI: 10.1016/j.scitotenv.2010.11.007.

- 26 P. Mikuška and Z. Večeřa, Effect of Complexones and Tensides on Selectivity of Nitrogen Dioxide Determination in Air with a Chemiluminescence Aerosol Detector, *Anal. Chim. Acta*, 2000, **410**(1–2), 159–165, DOI: **10.1016/S0003-2670(00)00710-8**.
- 27 DEFRA, Clean Air Strategy, 2019, p. 109.
- 28 C. Fàbrega, L. Fernández, O. Monereo, A. Pons-Balagué, E. Xuriguera, O. Casals, A. Waag and J. D. Prades, Highly Specific and Wide Range NO2 Sensor with Color Readout, ACS Sens., 2017, 2(11), 1612–1618, DOI: 10.1021/ acssensors.7b00463.
- 29 M. Cerrato-Alvarez, S. Frutos-Puerto, P. Arroyo, C. Miró-Rodríguez and E. Pinilla-Gil, A Portable, Low-Cost, Smartphone Assisted Methodology for on-Site Measurement of NO2 Levels in Ambient Air by Selective Chemical Reactivity and Digital Image Analysis, Sens. Actuators, B, 2021, 338, 129867, DOI: 10.1016/ j.snb.2021.129867.
- 30 J. Passaretti Filho, J. F. da Silveira Petruci and A. A. Cardoso, Development of a Simple Method for Determination of NO 2 in Air Using Digital Scanner Images, *Talanta*, 2015, **140**, 73–80, DOI: **10.1016/j.talanta.2015.03.009**.
- 31 Y. Tian, X. Zhang, H. Shen, A. Liu, Z. Zhao, M.-L. Chen and X.-W. Chen, High Time-Resolution Optical Sensor for Monitoring Atmospheric Nitrogen Dioxide, *Anal. Chem.*, 2017, 89(24), 13064–13068, DOI: 10.1021/ acs.analchem.7b03578.
- 32 J. P. Filho, M. A. M. Costa and A. A. Cardoso, A Micro-Impinger Sampling Device for Determination of Atmospheric Nitrogen Dioxide, *Aerosol Air Qual. Res.*, 2019, 19(11), 2597–2603, DOI: 10.4209/aaqr.2019.06.0318.
- 33 Y. Y. Maruo, M. Nakamura, Y. Higashijima, Y. Kikuya and M. Nakamura, Development of Highly Sensitive Nitrogen Dioxide Monitoring Device and Its Application to Wide-Area Ubiquitous Network, *Sens. Actuators, B*, 2012, 173, 191–196, DOI: 10.1016/j.snb.2012.06.075.
- 34 F. P. Scaringelli, E. Rosenberg and K. A. Rehme, Comparison of Permeation Devices and Nitrite Ion as Standards for the Colorimetric Determination of Nitrogen Dioxide, *Environ. Sci. Technol.*, 1970, 4(11), 924–929, DOI: 10.1021/es60046a003.
- 35 Standard Test Method for Nitrogen Dioxide Content of the Atmosphere (Griess-Saltzman Reaction), https://www.astm.org/d1607-91r18e01.html, accessed 2022-08-17.
- 36 R. H. Groth and D. S. Calabro, Evaluation of Saltzman and Phenoldisulfonic Acid Methods for Determining NOx in Engine Exhaust Gases, *J. Air Pollut. Control Assoc.*, 1969, 19(11), 884–887, DOI: 10.1080/00022470.1969.10469354.
- 37 A. Danielis, M. Guarneri, M. Francucci, M. Ferri De Collibus, G. Fornetti and A. Mencattini, A Quadratic Model with Nonpolynomial Terms for Remote Colorimetric Calibration of 3D Laser Scanner Data Based on Piecewise Cubic Hermite Polynomials, *Math. Probl. Eng.*, 2015, e606948, DOI: 10.1155/2015/606948.
- 38 A. M. Bica, Fitting Data Using Optimal Hermite Type Cubic Interpolating Splines, *Appl. Math. Lett.*, 2012, 25(12), 2047–2051, DOI: 10.1016/j.aml.2012.04.016.

- 39 F. N. Fritsch and R. E. Carlson, Monotone Piecewise Cubic Interpolation, SIAM J. Numer. Anal., 1980, 17(2), 238-246, DOI: 10.1137/0717021.
- 40 S. Johnsen, How to Measure Color Using Spectrometers and Calibrated Photographs, J. Exp. Biol., 2016, 219(6), 772-778, DOI: 10.1242/jeb.124008.
- 41 Department for Environment, F. and R. A. (Defra), What is the Daily Air Quality Index?, Defra, UK, https://ukair.defra.gov.uk/air-pollution/daqi?view=more-info, accessed 2022-08-17.
- 42 J. R. Subba, C. Thammakhet, P. Thavarungkul and P. Kanatharana, Distributions of SO 2 and NO 2 in the Lower Atmosphere of an Industrial Area in Bhutan, J. Environ. Sci. Health, Part A: Toxic/Hazard. Subst. Environ. 2016, 51(14), 1278-1287, DOI: Eng., 10934529.2016.1215196.
- 43 E. Felix, L. Gidhagen, M. F. Alonso, E. P. Nahirny, B. L. Alves, D. Segersson and J. H. Amorim, Passive Sampling as a Feasible Tool for Mapping and Model Evaluation of the Spatial Distribution of Nitrogen Oxides in the City of Curitiba, Brazil, Air Qual., Atmos. Health, 2019, 12(7), 837-846, DOI: 10.1007/s11869-019-00701-z.

- 44 D. A. Levaggi, W. Siu and M. Feldstein, A New Method for Measuring Average 24-Hour Nitrogen Dioxide Concentrations in the Atmosphere, J. Air Pollut. Control 1973. 23(1), 30-33. DOI: 10.1080/ Assoc., 00022470.1973.10469744.
- 45 T. Bush, S. Smith, K. Stevenson and S. Moorcroft, Validation of Nitrogen Dioxide Diffusion Tube Methodology in the UK, Atmos. Environ., 2001, 35(2), 289-296, DOI: 10.1016/S1352-2310(00)00172-2.
- 46 Air Quality Expert Group, Nitrogen Dioxide Inthe United Kingdom, DEFRA, 2004.
- 47 K. L. Chan, D. Pöhler, G. Kuhlmann, A. Hartl, U. Platt and M. O. Wenig, Long Term NO2 Measurements in Hong Kong Using LED Based Long Path Differential Optical Spectroscopy, Atmospheric Techniques Discussions, 2011, 4(6), 6615-6642, DOI: 10.5194/amtd-4-6615-2011.
- 48 Department for Environment, F. and R. A. (Defra), Data https://uk-air.defra.gov.uk/data/, Archive, Defra, UK, accessed 2022-08-17.